Using finite element modelling to examine the flow process and temperature evolution in HPT under different constraining conditions

2014 IOP Conf. Ser.: Mater. Sci. Eng. 63 012041

(http://iopscience.iop.org/1757-899X/63/1/012041)

IOP Conf. Series: Materials Science and Engineering **63** (2014) 012041 doi:10.1088/1757-899X/63/1/012041

Using finite element modelling to examine the flow process and temperature evolution in HPT under different constraining conditions

P H R Pereira[1,a], R B Figueiredo[2], P R Cetlin[3] and T G Langdon[1,4]

[1] Materials Research Group, Faculty of Engineering and the Environment, University of Southampton, Southampton SO17 1BJ, UK
[2] Department of Materials Engineering and Civil Construction, Universidade Federal de Minas Gerais, Belo Horizonte 31270-901, MG, Brazil
[3] Department of Mechanical Engineering, Universidade Federal de Minas Gerais, Belo Horizonte 31270-901, MG, Brazil
[4] Departments of Aerospace & Mechanical Engineering and Materials Science, University of Southern California, Los Angeles, CA 90089-1453, U.S.A

E-Mail: [a] pedrohrpereira@gmail.com

Abstract: High-pressure torsion (HPT) is a metal-working technique used to impose severe plastic deformation into disc-shaped samples under high hydrostatic pressures. Different HPT facilities have been developed and they may be divided into three distinct categories depending upon the configuration of the anvils and the restriction imposed on the lateral flow of the samples. In the present paper, finite element simulations were performed to compare the flow process, temperature, strain and hydrostatic stress distributions under unconstrained, quasi-constrained and constrained conditions. It is shown there are distinct strain distributions in the samples depending on the facility configurations and a similar trend in the temperature rise of the HPT workpieces.

1. Introduction

The processing of metallic materials through severe plastic deformation (SPD) methods has been extensively performed in order to produce bulk solids having high strength and exceptionally small grain sizes [1]. High-pressure torsion (HPT) [2] is an SPD technique especially effective in the fabrication of ultrafine-grained materials with grain sizes in the nanometer range. During the HPT processing a sample, usually in the form of a thin disc, is placed between massive anvils which are forced together and then rotate against each other with a given angular velocity imposing very high torsional straining and hydrostatic stresses in the workpiece.

The first experiments on processing by HPT were presented by Professor P. W. Bridgman in a classic paper published in 1943 [3]. Bridgman twisted a hollow

specimen while a longitudinal compressive load was simultaneously applied, such that it was possible to twist the sample through much greater angles without fracture than in the absence of compressive load. In the apparatus utilized by Bridgman there were no mechanical restrictions to the radial flow of the material during processing and the thinning and the outflow of the specimens was reported.

More recently, different HPT facilities were developed such that it is possible to divide HPT processing into three distinct groups depending upon the configuration of the anvils and restriction imposed on the lateral flow of the disc [2,4]. These categories are termed constrained, quasi-constrained and unconstrained HPT. In unconstrained HPT, the anvils are flat and the sample flows laterally without any mechanical restriction. Also, there is a pronounced thinning of the HPT disc during processing. On the other hand, in constrained HPT there is a physical barrier which prevents the lateral outflow of the processed material, however higher torsional torques are generally required using this HPT configuration [4]. In practice, HPT is generally conducted using a quasi-constrained condition in which the disk is placed between depressions in the upper and lower anvils and these partial lateral walls constrain the sample but permit some radial flow of material between the two anvils.

Although there are many reports using finite element modelling (FEM) to examine the temperature evolution [5-7] and the flow process in quasi-constrained HPT [8-10] and in unconstrained HPT [11,12] only a limited number of studies has been conducted concerning a comparison of the mechanical properties of the deformed HPT discs under different constraining conditions [4].

The present research was therefore initiated in order to compare the flow process, temperature, strain and hydrostatic stress distributions in HPT processing under unconstrained, quasi-constrained and constrained conditions.

2. Materials and Methods

Simulations were performed using the DEFORM 2D 10.0 software (Scientific Forming Technologies Corporation, Columbus, OH) and incorporated both the plastic deformation and the thermal evolution during HPT processing under different constraining conditions. Since there is axial symmetry around the central axis in HPT processing, the calculations were simplified by considering a two-dimensional model using only the axial and radial directions. The geometries of the anvils and the workpiece utilized in this study are depicted in Fig. 1.

As presented in Fig. 1, three different HPT facilities, similar to those illustrated in a previous study [4], were employed in order to simulate the HPT processing under unconstrained, quasi-constrained and constrained conditions. Regardless of the configuration of the HPT facilities, the samples are 10 mm in diameter with an initial thickness of 0.8 mm and the volume of each anvil is ≈58,200 mm^3.

In the unconstrained HPT, a hollow cylinder was used in addition to the anvils in order to prevent the lateral flow of the discs during the HPT simulations. Although no lateral flow was allowed using this facility configuration, there is a small gap of 0.05 mm between the hollow cylinder and the anvils which permits a limited vertical flow of the samples toward this narrow opening throughout the process.

It is also shown in Fig. 1 that, in quasi-constrained HPT, the anvils are 50 mm in diameter and 30 mm in height. They have shallow central depressions on their outer

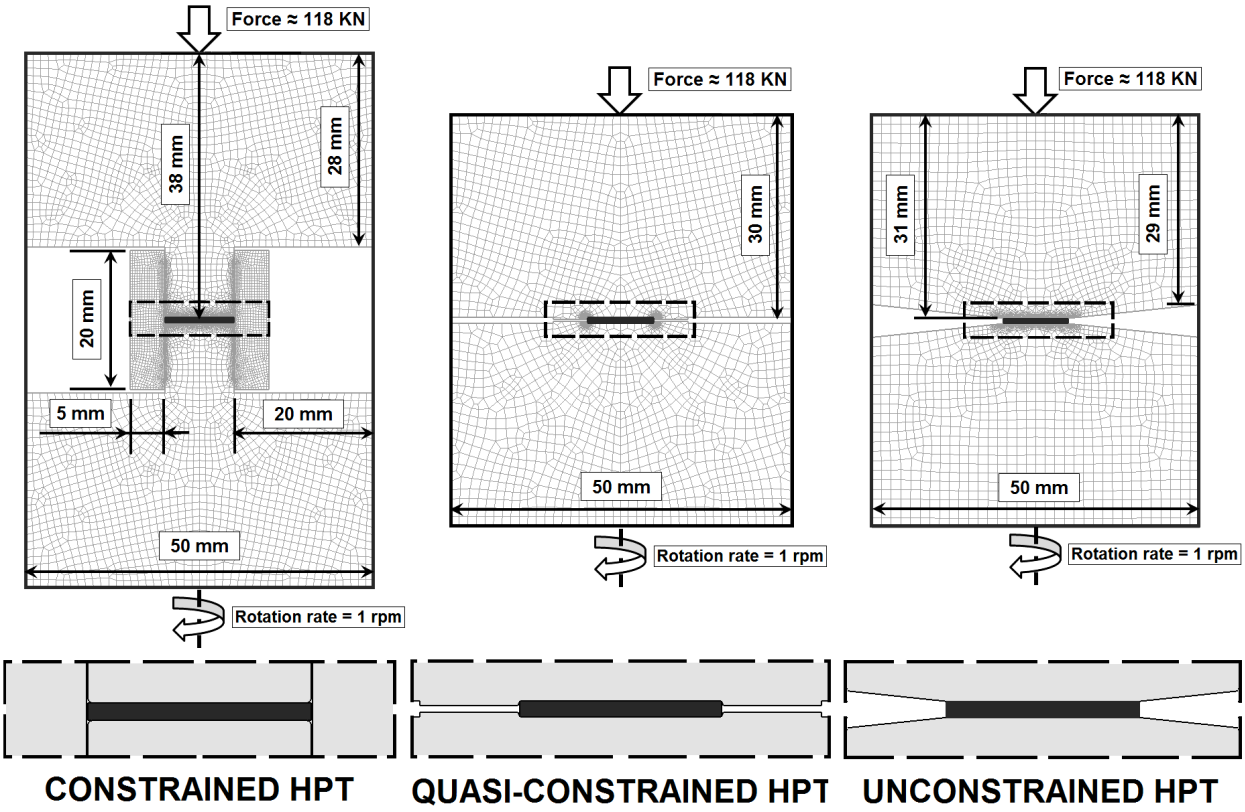

Fig. 1: Illustration of the geometry of the anvils and details of the geometry of the workpieces used in the simulations of the HPT processing under different constraining conditions.

surfaces, with depths of 0.25 mm and diameters of 10 mm at the bottom, and with slightly inclined walls having outer inclinations of ≈22°. The inclined anvil walls play an important role in quasi-constrained HPT processing since they constrain the material outflow and also allow the application of high hydrostatic stresses in the workpieces. On the other hand, the anvils employed in the simulation of the unconstrained HPT do not have shallow central depressions such that there is no restriction to the lateral outflow of the HPT disc.

Meshes were generated with ≈2200 elements in the workpiece, ≈1500 elements in each anvil and ≈1000 elements in the hollow cylinder utilized in the constrained HPT. A force of ≈118 KN was applied to the top anvils where this corresponds to a nominal pressure of 1.5 GPa. Both, the lower anvil and the hollow cylinder were set to rotate at constant rates of, respectively, 1.0 and 0.5 rpm, in a clockwise direction when seen from the top of the HPT apparatus. The simulations considered sticking conditions between the sample and the anvils on the top and bottom surfaces which means no slippage was allowed at these surfaces. A coefficient of friction of 0.8 [13,14] was considered in the contact between the sample and the anvils in the area of material outflow as well as in the contact between the anvil and the hollow cylinder in the simulation of the constrained HPT.

In the present simulations, it was considered that the temperature rise, ΔT, during plastic deformation is given by the following relationship [15]:

$$\Delta T = \frac{0.9}{C}\int \sigma \, d\varepsilon \quad (1)$$

where C is the heat capacity of the sample ($C=\rho C_p$ where ρ is the density and C_p is the specific heat capacity), σ is the flow stress, ε is the plastic deformation and the fraction of plastic deformation work converted into heat is assumed as 0.9.

It was considered that the anvils are rigid bodies with the thermal properties of tool steel. Both thermal conductivity and heat capacity adopted to the anvils were taken from the DEFORM software library and their values are, respectively, 42 $W\,m^{-1}\,K^{-1}$ and 3.72 $MJ\,m^3\,K^{-1}$. Before processing, the HPT facilities and discs were at the assumed room temperature of 24 °C (≈297 K) and a coefficient of heat convection of 50 $W\,m^{-2}\,K^{-1}$ was used in the simulations to take into account the loss of heat to the environment and to the remaining equipment. The thermal conductivity between the anvils and the workpiece was modelled using a value of 11 $W\,m^{-1}\,K^{-1}$, as recommended by the DEFORM software for die-workpiece contacts in metal–forming operations and used in previous works on the modelling of the temperature rise in HPT [6,7].

The material of the workpiece was commercially pure copper with thermal conductivity of 401 $W\,m^{-1}\,K^{-1}$ and thermal capacity of 3.45 $MJ\,m^3\,K^{-1}$ [16]. Based on the stress vs. strain curve of a previous study [17] obtained from the torsion testing of a commercially pure copper, a Voce-type equation [18] was adopted to describe properly the flow stress of the workpiece in a wide range of strains. The adjusted Voce-type equation is presented in Eq. (2), where σ and ε are, respectively, the effective stress and the effective strain.

$$\sigma = 460 - 276e^{-0.8\varepsilon} \quad (2)$$

3. Results

3.1. Distribution of effective strain in the HPT samples

Figure 2 shows the shape and the distribution of effective strain on the cross-sections of discs after one turn of processing by HPT with the nominal pressure, P_{nom}, of 1.5 GPa and the rotation rate, n, of 1.0 rpm. As presented in Fig. 2, the distribution of strain is

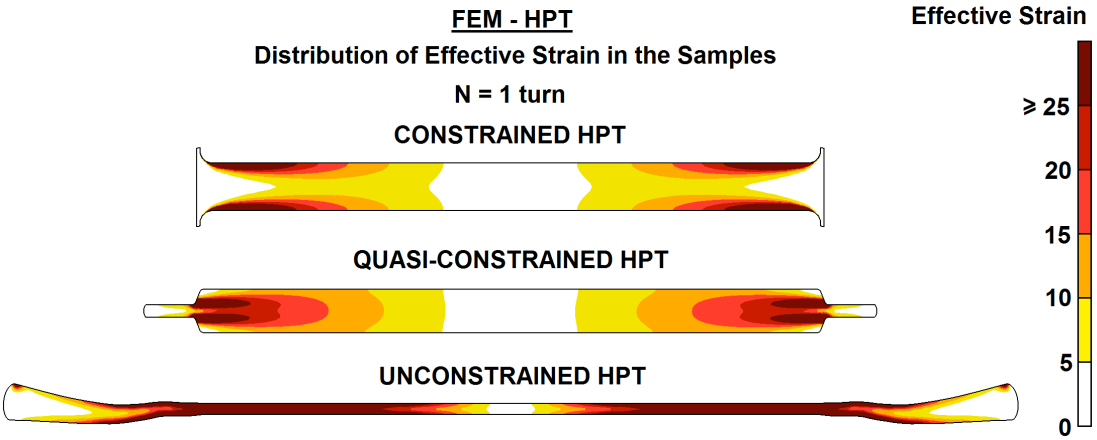

Fig. 2: Distribution of effective strain across the cross-sectional planes of discs after one turn of processing by HPT using different constraining condition. The nominal pressure imposed in the samples was 1.5 GPa and the rotation rate of the lower anvil was 1.0 rpm.

highly heterogeneous in HPT discs, regardless of the configuration of the facilities employed in the FEM simulations.

In constrained HPT, the highest values of strain are found in the upper and lower surfaces of the disc near its periphery, where the effective strain is greater than 25. The lower values of strain are found in the middle section of the disc near its geometrical centre and in the region where the disc was in contact with the hollow cylinder during processing. It is observed that there was a slight thinning of the disc after 1 turn of HPT and material was able to outflow into the gap between anvils and the hollow cylinder, as experimentally verified [4].

In unconstrained HPT, there is a considerable thinning of the disc during processing. The thickness of the sample is ≈0.18 mm and a thick and large ribbon is formed after 1 turn of HPT. As a consequence of the severe thinning of the specimen, the effective strain in its cross-section is greater than 25, except near the centre and in the ribbon of the sample.

Figure 2 also reveals that, after one turn of processing by quasi-constrained HPT, the thickness of the copper sample is ≈0.7 mm and there is the formation of a thin extruded ribbon around the middle periphery of the disc. The strain increases with increasing distance from the centre of the disc and it is very heterogeneous in the vicinity of the lateral edges, where the highest strains are achieved near their inner corners.

3.2. Distribution of hydrostatic stress in the HPT samples

Figure 3 shows the distribution of hydrostatic stress on the cross-sections of discs after one turn of processing by HPT. A compressive load of ≈118 KN was applied in the workpiece by the upper anvil during processing with all HPT configurations. Since the initial area of the samples is ≈78.54 mm^2, P_{nom} is ≈1.5 GPa and it is expected that the workpiece would undergo a hydrostatic stress of -1.5 GPa in the absence of any material outflow.

As shown in Fig. 3, after one turn of processing by constrained HPT the distribution of hydrostatic stress in the copper specimen is homogenous and the hydrostatic stresses are in the range of -1980 to -1320 MPa. A more detailed examination of the simulation results for this HPT facility reveals that the hydrostatic stress is ≈-1.5 GPa in

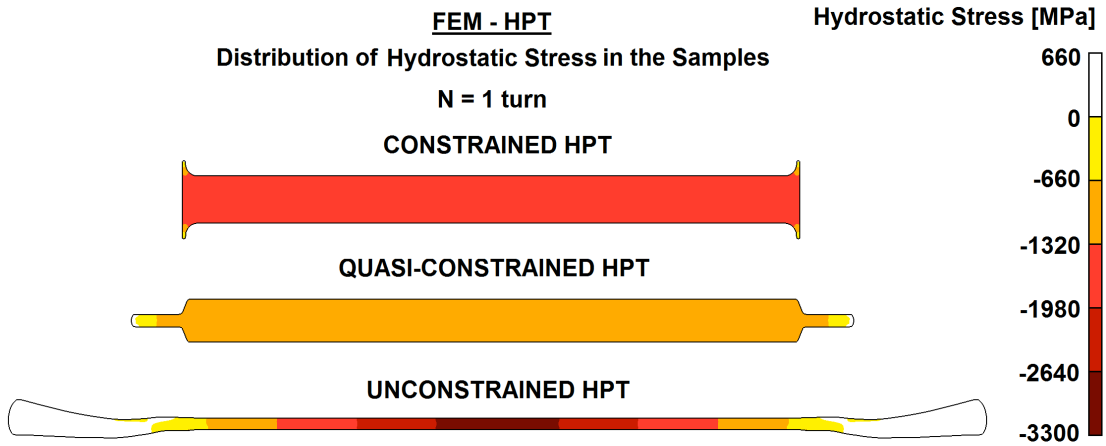

Fig. 3: Distribution of hydrostatic stress across the cross-sectional planes of discs after one turn of processing by HPT using different constraining condition. The nominal pressure imposed in the samples was 1.5 GPa and the rotation rate of the lower anvil was 1.0 rpm.

the entire HPT disc, except in the thin ribbon formed between anvils and the hollow cylinder.

In quasi-constrained HPT, after one turn of HPT, the hydrostatic stresses in the workpiece are in the range of -1300 to -700 MPa. Despite the hydrostatic stress of ≈ -1.2 GPa in the cross-section of the disc, the distribution of hydrostatic stress is also very homogeneous along the sample radius and thickness, as in specimens processed by constrained HPT.

It is observed in Fig. 3 that the distribution of hydrostatic stress is significantly heterogeneous in the disc processed by unconstrained HPT. The most negative values of stresses are found in the centre of the sample and it is apparent that the absolute value of the hydrostatic stresses increase, increasing the sample radius. Positive values of hydrostatic stress are found in the ribbon region as expected since there is no mechanical restriction to the ribbon growth.

3.3. Temperature rise in the HPT samples

The evolution of temperature in the discs during processing by HPT is presented in Fig. 4. It is verified that the distribution of temperature in the cross-section of the copper samples is very homogeneous, regardless of the numbers of turns and the configuration of the HPT facilities.

In the beginning of the HPT processing the temperature of the samples was 24 °C. After 1 turn of HPT, one can see a rapid temperature rise in the workpieces such that, in constrained HPT, this temperature is between 36 to 40 °C, whereas in the quasi-constrained and unconstrained samples it is in the range of 32 to 36 °C. After 20 turns, the samples processed by constrained and quasi-constrained HPT are in the same

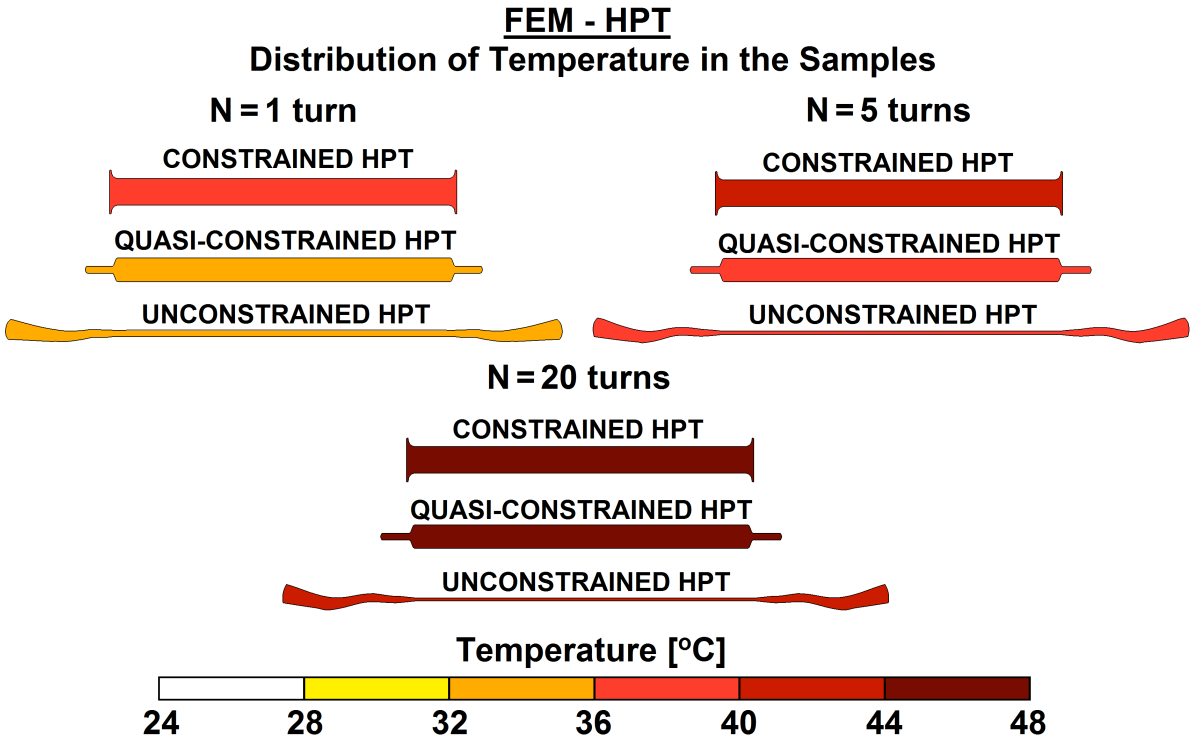

Fig. 4: Evolution of temperature across the cross-sectional planes of discs during processing by HPT using different constraining condition. The nominal pressure imposed in the samples was 1.5 GPa and the rotation rate of the lower anvil was 1.0 rpm.

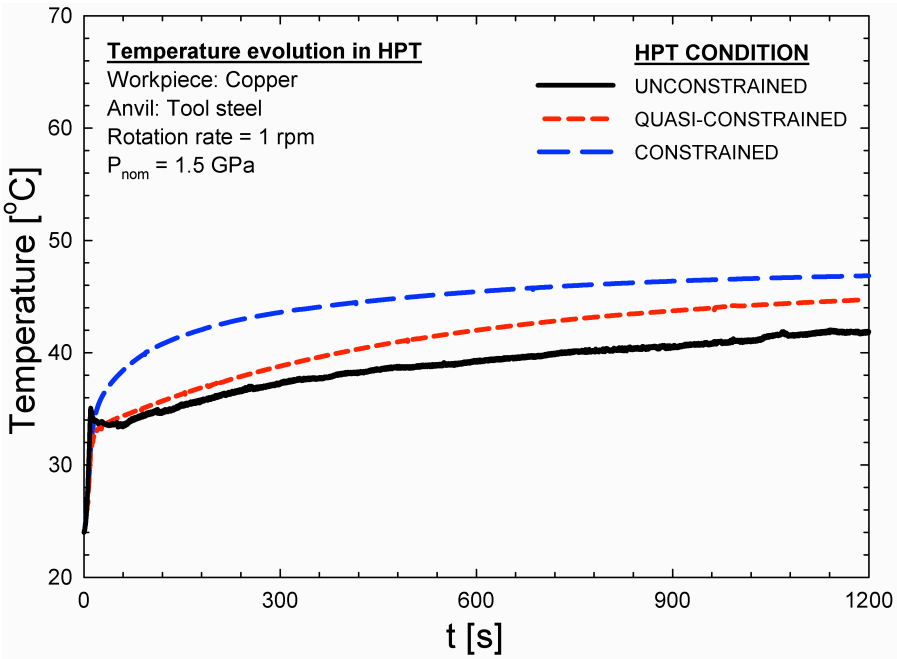

Fig. 5: Variation of temperature as a function of time in HPT discs of copper processed at a rotation rate of 1.0 rpm using different constraining conditions.

range of temperatures while the temperature in the disc processed by an unconstrained HPT facility is slightly lower.

Figure 5 shows the evolution of temperature in the workpieces during HPT processing at a rotation rate of 1.0 rpm using different constraining conditions. It is shown in Fig. 5 that all HPT simulations present the same general trend. There is a sudden increase in the temperature of the samples of about 10 °C. Thereafter, the temperature of the samples continuously increase, but at lower rates and, ultimately, a saturation temperature is achieved in the HPT discs.

It is observed that the initial rate of temperature rise is higher in the simulation of constrained HPT leading to greater values of temperature in this sample when compared with the samples processed using other HPT configurations. Nevertheless, after 20 turns (1200 s) of processing by HPT, the temperatures in the samples are very similar varying from 42 °C in unconstrained HPT to 46 °C in constrained HPT.

It is worth noting that in the beginning of the HPT processing the difference of temperature in the workpieces processed in quasi-constrained and unconstrained HPT is negligible, however increasing the numbers of turns this difference grows and, after 1200 s this difference is near to 2 °C.

4- Discussion

4.1. Distribution of effective strain in the HPT samples

The simulations results presented in Fig. 2 reveal that the flow process in HPT processing with different constraining conditions is very dissimilar even using the same nominal pressure and rotation rate.

Analysing the distribution of effective strain in the cross-sectional plane of the sample in the simulation of constrained HPT, there is evidence for flow localization in the vicinity of the surfaces of the anvils where there is no sliding between the anvils

and the workpiece. It is also apparent that the magnitude of the effective strain increases with increasing distance from the centre of the disk.

As was established in the constrained HPT simulation, the rotation rate of the lower anvil and the tube are constant and equal to 1.0 and 0.5 rpm during processing. Therefore, because of the high hydrostatic stresses and the high coefficient of friction of the copper specimen, there is no tangential sliding between the lateral surface of the copper specimen and the inner wall of the hollow cylinder and the rotation rate of the sample in the vicinity of the tube is ≈0.5 rpm. Also, a zone of restricted flow is formed in the workpiece as a consequence of the friction in the inner surface of the tube which explains the region with low plastic strains observed next to the flow localization zone.

It is also observed there is the formation of a very thin ribbon which flows vertically during the constrained HPT simulation. It is thought that the length of this ribbon depends upon the coefficient of friction of the workpiece, the rotation rate of the anvil and the tube, as well the nominal pressure utilized.

In quasi-constrained HPT, it is verified that the plastic strain also increases with increasing distance from the centre of the disk and it concentrates close to the outer corners of the lateral walls of the anvils. The through-thickness deformation is highly inhomogeneous near the lateral edges of the workpiece due to the presence of severe deformed regions near its middle-section and the formation of a dead zone at its upper and outer corners, as shown elsewhere [4,10]. A thin ribbon is also formed in the middle-section of the sample as a consequence of its thinning and the partial restriction to its radial flow made by the anvil depression walls.

The absence of a mechanical restriction to the material outflow in unconstrained HPT and the compressive load applied by the upper anvil lead to a significant thinning of the HPT sample and the formation of a thick and large ribbon. As is observed in Fig. 4, the overall shape of the HPT discs does not change significantly from 1 turn to 20 turns of processing which indicates that the compression stage of the samples plays an important role regarding the shape of the samples and the size of their ribbons independent of the HPT constraining condition.

Since the ribbon is formed in the very beginning of processing in unconstrained HPT and the thickness to diameter ratio of the sample is lower when compared with the samples processed using quasi-constrained and constrained facilities, it is expected there will be a more uniform distribution of strain along the thickness of the disc in unconstrained HPT as suggested elsewhere [4,9] and confirmed in the present simulations.

4.2. Distribution of hydrostatic stress in the HPT samples

As indicated in Fig. 3, the distribution of hydrostatic stress is very homogeneous after 1 turn of processing by HPT using facilities which prevent, at least partially, the material outflow. It is also observed that the absolute value of hydrostatic pressure is very close to the nominal value in fully constrained samples and is somewhat lower in quasi-constrained HPT. As the load applied by the upper anvil remains constant during processing, this difference can be related to the increase in the surface area of the sample surface as a consequence of the material outflow in quasi- constrained HPT.

On the other hand, the copper disc processed using unconstrained HPT exhibits a pronounced gradient of stress along the radial direction. Since the only restriction to

the radial outflow of the sample in unconstrained HPT is the friction in the surface of the anvils, a friction hill [15] is formed in the workpiece. Consequently, it is verified that the absolute value of the hydrostatic stress is superior to the nominal pressure near the disc centre and is less at radii greater than 3 mm.

It is also evident in Fig. 3 that large regions with tensile stresses are found in the ribbon in unconstrained HPT because the surface of the ribbon is free to grow and it is not in contact with the upper and lower anvils.

4.3. Temperature rise in the HPT samples

Through the shaded contours depicted in Fig. 4, it is seen that the temperature in the HPT discs is very uniform, regardless of the number of turns and the configuration of the anvils. This means that even if the heat generation rate is very different across the sample during processing, the high conductivity of copper distributes rapidly the heat along the workpiece such that the temperature is almost the same in any position in the sample.

It is possible to observe in Fig. 5 that the temperature evolution in HPT with unconstrained, quasi-constrained and constrained conditions follow the same general trend described in recent reports [6,7]. There is an almost instantaneous temperature increase at the beginning of processing since a great amount of the heat generated due to the plastic straining remains in the workpiece region in the initial stage of HPT. Following this initial stage, the temperature gradient between the sample, the HPT apparatus and the environment leads to heat transfer so that the HPT facilities and the environment act as heat sinks and the temperature in the disc rises slowly until it reaches a saturation temperature.

The increasing difference in the temperature of the samples with the time of processing in quasi-constrained and unconstrained HPT may be explained based on the effect of friction in the ribbon region. The friction between the copper ribbon and the adjacent anvils leads to additional heating in the HPT discs with increasing numbers of turns. Hence, as the ribbon does not touch the anvils used in the present simulation of the unconstrained HPT, it is expected that the temperature in the sample will be slightly higher in quasi-constrained HPT.

A recent report suggested a simplified relationship to estimate the temperature rise in samples processed using a conventional quasi-constrained HPT facility [7]. This relationship was used in order to calculate the temperature rise in the present simulation. The values calculated for the temperature achieved after the initial temperature rise and the saturation temperature are, respectively, ≈34.5 °C and ≈48.0 °C, showing an excellent agreement with the FEM results presented in Fig. 5 since the difference between the FEM results and the values predicted by the simplified relationship is within 15%.

5. Summary and conclusions

Finite element modelling was used to compare the flow process, temperature, strain and hydrostatic stress distributions in HPT processing under unconstrained, quasi-constrained and constrained conditions.

The distribution of effective strain is highly heterogeneous in HPT discs in all simulations. It is observed that there are distinct regions of flow localization in samples

processed by constrained and quasi-constrained HPT and a more uniform distribution of strain along the thickness of the disc in unconstrained HPT.

The distribution of hydrostatic stress is very homogeneous and close to the nominal pressure after processing by HPT using constrained and quasi-constrained facilities. On the other hand, in unconstrained HPT, there is a pronounceable gradient of stress along the radial direction.

The temperature evolution in HPT with unconstrained, quasi-constrained and constrained conditions follow the same general trend. There is good agreement between the FEM results and a simplified relationship developed recently to predict the temperature evolution in HPT [7].

Acknowledgements

This work was supported by CNPq, FAPEMIG, CPGEM, CAPES under Agreement No. PVE 037/2012 and the European Research Council under ERC Grant Agreement No. 267464-SPDMETALS.

References

[1] Valiev R Z, Islamgaliev R K and Alexandrov I V 2000 *Prog. Mater. Sci.* **45** 103
[2] Zhilyaev A P and Langdon T G 2008 *Prog. Mater. Sci.* **53** 893
[3] Bridgman P W 1943 *J. App. Phys..* **14** 273
[4] Hohenwarter A, Bachmaier A, Gludovatz B, Scheriau S and Pippan R 2009 *Int. J. Mat. Res.* **100** 1653
[5] Edalati K, Miresmaeili R, Horita Z, Kanayama H and Pippan R 2011 *Mater. Sci. Eng. A* **528** 7301
[6] Figueiredo R B, Pereira P H R, Aguilar M T P, Cetlin P R and Langdon T G 2012 *Acta Mater.* **60** 3190
[7] Pereira P H R, Figueiredo R B, Huang Y, Cetlin P R and Langdon T G 2014 *Mater. Sci. Eng. A* **593** 185
[8] Figueiredo R B, Cetlin P R and Langdon T G 2011 *Mater. Sci. Eng. A* **528** 8198
[9] Figueiredo R B, Aguilar M T P, Cetlin P R and Langdon T G 2012 *J. Mater. Sci.* **47** 7807
[10] Lee D J, Yoon E Y, Park L J and Kim H S 2012 *Scripta Mater.* **67** 384
[11] Kim H S 2001 *J. Mater. Process. Technol.* **113** 617
[12] Kim H S, Hong S I, Lee Y S, Dubravina A A and Alexandrov I V 2003 *J. Mater. Process. Technol.* **142** 334
[13] Zhang Y S, Wang K, Han Z and Liu G 2007 *Wear* **262** 1463
[14] Zhilyaev A P, Shakhova I, Belyakov A, Kaibyshev R and Langdon T G 2013 *Wear* **305** 89
[15] Hosford W F and Caddell R M 2007 Metal Forming: Mechanics and Metallurgy (3 ed.) Cambridge University Press (New York)
[16] 1990 Metals Handbook: Properties and Selection on Non-ferrous Alloys and Special-Purpose Materials (vol. 2) ASM International (Metals Park, OH)
[17] Figueiredo R B, Pinheiro I P, Aguilar M T P, Modenesi P J and Cetlin P R 2006 *J. Mater. Process. Technol.* **180** 30
[18] Voce E 1948 *J. Inst. Met.* **74** 537